metals

MDPI

Review

Review on Grain Refinement of Metallic Materials to Regulate Cellular Behavior

Yingjian Gu [1], Run Huang [1,2,*] and Yufei Hao [1]

[1] School of Materials Science and Engineering, Anhui University of Science and Technology, Huainan 232001, China; gu_yjian@163.com (Y.G.); talnothyf@163.com (Y.H.)
[2] Institute of Environment-Friendly Materials and Occupational Health, Anhui University of Science and Technology (Wuhu), Wuhu 241003, China
* Correspondence: runhuang@aust.edu.cn; Tel.: +86-0554-6668201

Abstract: Metallic materials have been widely used as orthopedic implants in clinics for their good mechanical, physical, and chemical properties, but their slow osseointegration rate is still one of the main issues causing implantation failure. Grain refinement has recently attracted wide attention for its effective improvement of cell–material interaction for biometals. In this review, the surface and bulk grain refinement mode and the influence of grain size reduction of various metallic materials including titanium, stainless steel, magnesium, zirconium, tantalum, and their alloys as well as NiTi shape memory alloys on the cell responses is summarized in detail. It is hoped that this review could help biomaterials-related researchers to understand the grain refinement of metallic materials in a timely manner, thus boosting the development of biomedical metals for clinical use.

Keywords: metals; grain size; implants; cell response

Citation: Gu, Y.; Huang, R.; Hao, Y. Review on Grain Refinement of Metallic Materials to Regulate Cellular Behavior. *Metals* **2022**, *12*, 829. https://doi.org/10.3390/met12050829

Academic Editor: Alexander Tsouknidas

Received: 20 March 2022
Accepted: 1 May 2022
Published: 11 May 2022

1. Introduction

Currently, metallic materials such as titanium, stainless steel, magnesium, etc. are widely used in the fields of orthopedics and dentistry because of the superior mechanical properties (e.g., high tensile strength, toughness, and fracture resistance) compared with the ceramics and bio-glass [1,2]. Some typical applications of the metallic materials are shown in Figure 1.

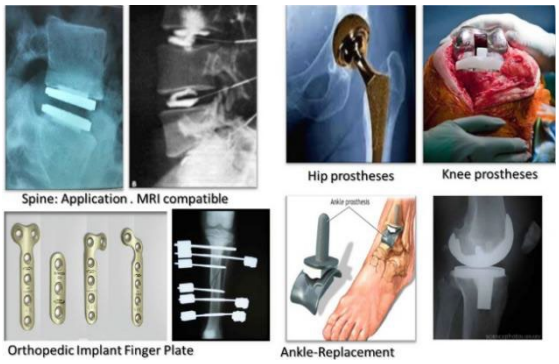

Figure 1. Metallic biomaterials for orthopedic applications reprinted with permission from Ref. [1]. Copyright 2022, ELSEVIER.

However, for materials implanted into the body, it is important to ensure that they do not have negative effects; Willams defined this idea of biocompatibility as "the ability of a biomaterial to perform its desired function with respect to a medical therapy, without eliciting any undesirable local or systemic effects in the recipient or beneficiary of that therapy, but generating the most appropriate beneficial cellular or tissue response to that specific

situation, and optimizing the clinically relevant performance of that therapy" [3]. In order to improve biocompatibility, predecessors have used micro-arc oxidation, hydrothermal synthesis, thermal spraying, electroless plating, and other methods to form a biologically active surface layer (usually a ceramic surface layer) on the metal surface [4–6]. Nevertheless, there is a problem: the interface between these heterogeneous coatings and the substrate can easily peel off. In this regard, severe plastic deformation (SPD)—a technique which can fabricate metals with ultrafine-grained (UFG) or nano-grained (NG) structure—shows great potential in the field of biomedicine [7–10]. It has been reported that SPD-derived ultra-/nano-structures possess a large fraction of grain boundaries and more lattice imperfections such as dislocations, vacancies, stacking faults, and twins, which has the positive effect of improving the mechanical properties (particularly the strength, according to the Hall-Petch theory) and increasing the surface energy of the metals to mediate protein adsorption, thus benefiting the subsequent cell response and tissue growth [11,12].

In general, the SPD method can refine the coarse-grained materials into UFG or NG materials through two modes: one is applying high strain on the material's surface to generate surface grain refinement, and the other is using extremely high plastic deformation to compel the whole grain size of the bulk materials to reduce into the UFG or NG regime. In recent years, these two modes—including surface mechanical attrition treatment (SMAT), ultrasonic shot peening (USSP), friction stir processing (FSP), and equal channel angular pressing (ECAP)—have been used extensively to surface/bulk modify the metals in order to avoid the interface bonding issue (shown in Figure 2) and improve biocompatibility.

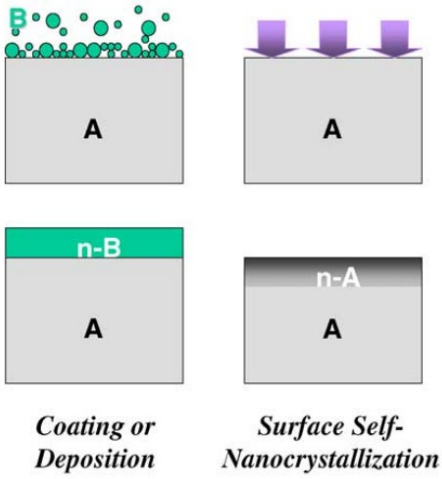

Figure 2. Schematic illustrations of (**A**) surface coating and (**B**) surface nano-crystallization reprinted with permission from Ref. [13]. Copyright 2022, ELSEVIER.

For example, Agrawal et al. [14] used USSP to obtain a layer with an average grain size of about 20 nm on the surface of pure titanium and found that human mesenchymal stem cells (hMSCs) exhibited better cell viability on the nano-grained samples. Bahl et al. [15] fabricated a nanocrystalline layer with an average size of about 40 nm on the cp-Ti by SMAT; after 14 days of cell culture, the proliferation rate of hMSCs was observed to be higher on the NC (nanocrystalline) surface compared with the MC (microcrystalline) surface. In addition, the ECAP-treated titanium alloy was reported to not only possess better antibacterial properties, but also promote the differentiation of human fetal osteoblast (hFOB) cells, while the grain size reduced to 500–700 nm [16]. In view of the strong capability to endow metallic materials with better biocompatibility, together with the coherence of substrate and surface layers, these methods represent a potential route for developing new types of implants to be used in clinics.

In this paper, the status of recent research on surface/bulk grain refinement of metallic materials to improve the biological activity is summarized, and some opinions and prospects are put forward in relation to this field. Through the summary, we hope the

research progress of the development of biomaterials in this field can be accelerated, thereby promoting wider clinical application of metallic materials in the near future.

2. Two Grain Refinement Modes for Treating Metallic Materials

2.1. Surface Grain Refinement

2.1.1. Surface Mechanical Attrition Treatment (SMAT)

Surface mechanical attrition treatment (SMAT) is a physical modification method for obtaining new gradient nanometal materials [17]. It is an effective method for achieving the surface nanocrystallization of many metals, such as titanium, aluminum, nickel, steel, magnesium, and copper. The basic process is summarized as follows: Smooth spheres made of steel or ceramic, with a diameter of 3–10 mm, are placed in a chamber which is connected to a vibration generator. The vibration frequency of the chamber is 50 Hz and 20,000 Hz for I-type and II-type SMAT techniques, respectively [18]. The sample surface to be treated is impacted by a large number of balls in a short period of time, with a velocity of 1–20 m/s depending on the vibration frequency and the distance between the sample surface and the balls [13]. The impact of each ball causes severe plastic deformation (SPD) on the surface layer and facilitates the process of nanocrystallization. The thickness of the nanostructured surface layer depends very much on the processing parameters (such as ball size, vibration frequency, temperature, etc.) [13]. With flexibility and low cost, SMAT can obtain localized nanostructured surface layers in bulk materials and is capable of treating the surfaces of parts with complex shapes. In addition, this technique can produce surfaces with low roughness because of the better quality of shots and a lower impact speed [11]. The SMAT process is illustrated in Figure 3.

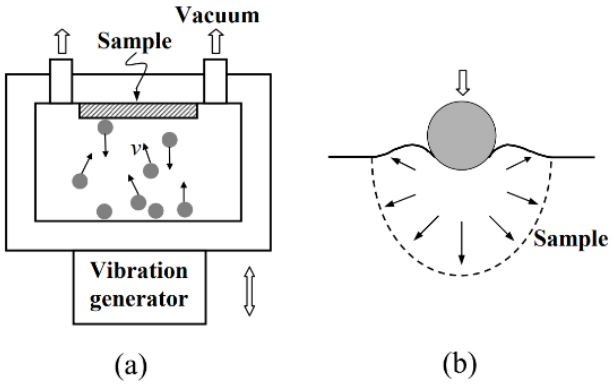

Figure 3. Schematic illustrations of the (**a**) SMAT setup and (**b**) localized plastic deformation in the surface layer of the treated sample, caused by the impact of balls reprinted with permission from Ref. [19]. Copyright 2022, ELSEVIER.

2.1.2. Ultrasonic Shot Peening (USSP)

The ultrasonic shot peening (USSP) process is a kind of shot peening. It can optimize the characteristics of the material surface, modify the material properties, and improve the wear and fatigue resistance. A power ultrasonic horn causes impacts with high frequency (generally higher than 20 kHz) and low amplitude. The whole process is quiet because it operates more frequently than the human ear can perceive. The high-frequency and multi-directional shock acts on the surface randomly, creating a kind of microdimple shape and forming a nanocrystalline surface layer. USSP treatment is an effective approach for forming a nanostructure layer on the surface of metallic materials [20]. However, the relatively high strain might result in residual porosities, impurities, and dimensional issues [21]. The main structure of USSP is displayed in Figure 4.

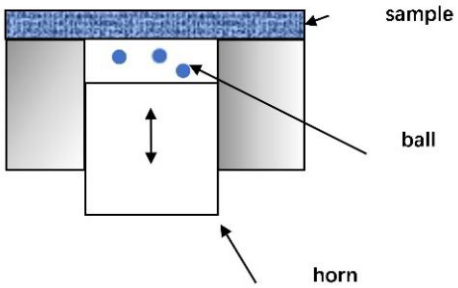

Figure 4. Schematic illustrations of the USSP process.

2.1.3. Laser Shock Peening (LSP)

Laser shock peening (LSP) is a surface modification process that uses laser beams to generate shock waves on the surface of a material. As shown in the Figure 5, a high-energy laser is emitted from the light source, reflected by the mirror, and irradiated on the surface of the sample after being focused. The continued delivery of laser pulses rapidly heats and ionizes the vaporized material, converting it into rapidly expanding plasma [22] while a shock wave is created. If the amplitude of the shock wave is above the Hugoniot elastic limit (HEL) of the target, the material deforms plastically during the passage of shock waves, resulting in compressive residual stresses below the target surface [22]. However, due to the thermal effect, LSP is less efficient in refining the surface grains compared to the mechanical treatments. The LSP process is expensive and takes a long time to scan a large area compared with other processes [23].

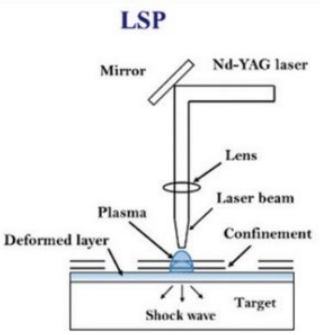

Figure 5. Schematic illustration of the LSP process reprinted with permission from Ref. [23]. Copyright 2022, Marketplace.

2.1.4. Friction Stir Processing (FSP)

FSP provides great flexibility in terms of processing conditions to tailor the localized microstructure in a material [24]. Its principle is similar to friction stir welding, which uses frictional heat to treat materials. The tool shoulder is fastened to the sample, and the tool pin is in close contact with the surface of material. As shown in the Figure 6, in the process of FSP, the tool pin rotates at high speed and moves to the specified direction; then, severe plastic deformation occurs on the surface of sample, which is called the stir zone. Due to high frictional heat and dynamic recrystallization [25], fine grains will be generated in the processing area. The main parameters influencing FSP are rotating speed, advancing speed, plunging force, etc. In addition, microstructure and mechanical properties will also be altered with respect to the geometry of tool and the materials it uses [26]. The strict requirements of the processing conditions are a major disadvantage of FSP, hindering extensive use of this technique. In addition, the relatively high temperature during the process makes it difficult to adapt it to the production of grain structures in the nanoscale regime [27].

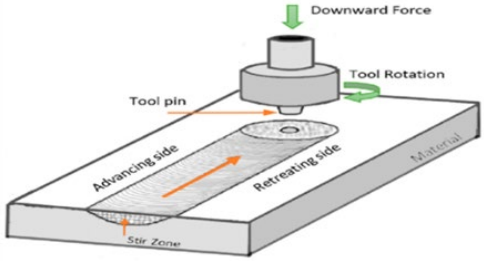

Figure 6. Schematic illustrations of the friction stir process reprinted from [26].

2.1.5. Ultrasonic Nanocrystal Surface Modification (UNSM)

The UNSM technique was developed and commercialized by Design Mecha Co., Ltd. (Seoul, South Korea). It is a mechanical impact-based surface treatment applied by means of high ultrasonic vibration frequency [28]. Its basic structure is shown in Figure 7. The process includes the settings of parameters such as frequency, input amplitude, interval, horn speed, and tip (ball) diameter. The spherical tip—made of hard Al_2O_3, WC, or Si_3N_4—impacts the surface at a specific frequency. The superposition of ultrasonic low-frequency vibration on static load causes severe plastic deformation on the surface of the material, inducing grain size decreases to the nanoscale. During this process, the sample is clamped on the gripper, which reciprocates up and down (Y direction) with a constant velocity. After each Z direction scan, the silicon nitride or tungsten carbide prompts it to move a constant distance in the Z direction [29]. After treatment, the coarse-grained structure in the surface layer of the sample is refined to the nanometer level, which corresponds to the characteristics of finer grains and more uniform dislocation distribution (Figure 8), forming a gradient nanostructure layer with a depth of several hundreds of microns [30,31]. Moon et al. [32] found that specimens treated with the UNSM process exhibited much higher tensile strength compared to untreated specimens.

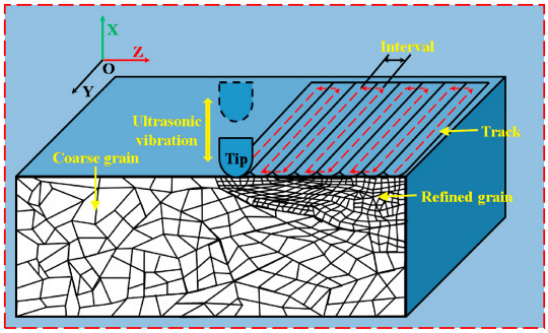

Figure 7. Schematic illustration of the UNSM process reprinted with permission from Ref. [29]. Copyright 2022, ELSEVIER.

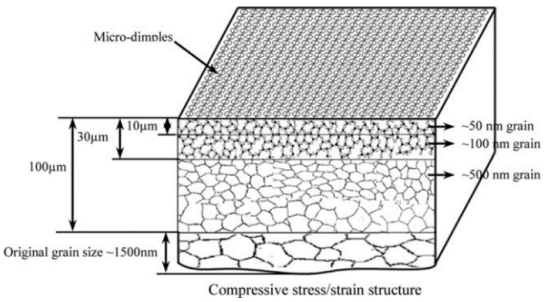

Figure 8. Schematic illustration of structure characteristics and distributions in a surface layer subjected to the UNSM reprinted with permission from Ref. [31]. Copyright 2022, ELSEVIER.

2.2. Bulk Grain Refinement

2.2.1. High-Pressure Torsion (HPT)

High-pressure torsion (HPT) refers to the processing of a metal which bears compressive force and simultaneous torsion force. As shown in Figure 9, the sample in this process is laid in the shape of a disc between two anvils. The sample is subjected to a squeezing pressure P of several GPa at room temperature; at the same time, it bears a torsion force generated by the rotation of the lower anvil [33,34]. Sometimes, in order to improve the HPT processing efficiency, the process needs to be carried out at a higher temperature; under this condition, the shearing and pressing speed should be controlled [35]. During HPT, the strain is allowed to continuously change, and it is easy to achieve high shear strains. Moreover, even materials that are relatively hard and brittle can undergo the severe deformation in this method [36].

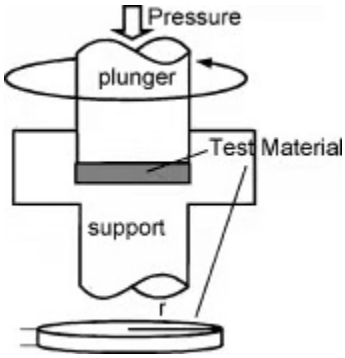

Figure 9. Schematic illustrations of the high-pressure torsion process reprinted with permission from Ref. [34]. Copyright 2022, ELSEVIER.

The disadvantage of HPT is that the process usually requires high pressure and torque; otherwise, it will cause a significantly inhomogeneous microstructure in the treated sample. Therefore, HPT cannot be utilized to produce large bulk materials.

2.2.2. Equal Channel Angular Pressing (ECAP)

Equal channel angular pressing (ECAP) has been one of the most important machining procedures in the past few decades. It was proposed by Segal in the 1970s at an institute in Minsk in the former Soviet Union [37].Before the process, the sample needs to be lubricated; it is then squeezed through two intersecting channels (equal section) and subjected to a shearing force at the intersection of the channels [38], as shown in Figure 10. The cross section of two equal-length channels is related to the angle φ (internal model/channel angle φ), whilst the angle ψ is the curvature arc at the intersection (outer curvature arc/external rotation angle ψ). The same sample is subjected to multiple extrusions, that is, repeated shear deformation; this causes a large amount of cumulative plastic strain in the material, resulting in obvious grain refinement [39]. Although the sample undergoes very strong strain when it passes through the shear plane, the cross-sectional dimension of the sample does not change, even when it finally comes out of the mold.

In the work conducted by R.Z. Valiev [40], the following routes of billets were considered: orientation of a billet is not changed at each pass (route A); after each pass, a billet is rotated around its longitudinal axis through the angle 90° in the same direction (route B_c) or inverse direction (route B_a); after each pass, a billet is rotated around its longitudinal axis through the angle 180° (route C). This process is displayed in Figure 11. Some researchers [41,42] have even pointed out that, compared with other pressing routes, the route B_c is more advantageous for obtaining ultra-fine grain (UFG) materials with a more uniform microstructure. ECAP is used to manufacture UFG structures among various SPD technologies and can produce large bulk materials for various applications, such as rod-shaped production for dental implants [43]. Additionally, ECAP can significantly

economize raw materials [44]. The main disadvantage of ECAP is that the process usually happens discontinuously, with limitations in scale-up potential [45].

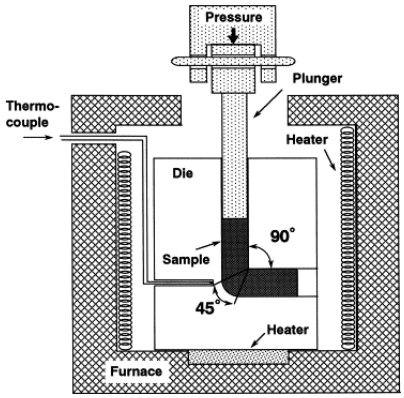

Figure 10. Schematic illustration of the ECAP reprinted with permission from Ref. [34]. Copyright 2022, ELSEVIER.

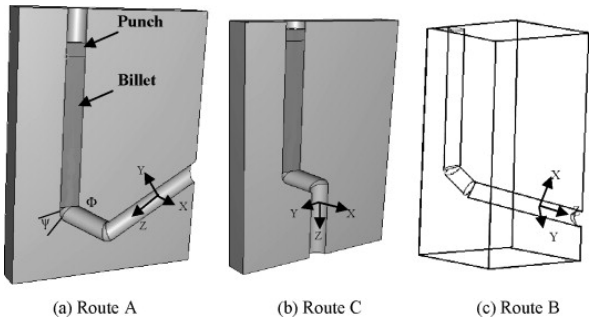

Figure 11. FEM (finite element method) models of ECAP reprinted with permission from Ref. [41]. Copyright 2022, ELSEVIER.

Based on ECAP, several variants have been developed to enhance its effect. A novel method proposed the application of vibrations with ultrasonic frequencies on the plunger to reduce the friction and forming load during ECAP; longitudinal ultrasonic vibrations were imposed onto the billet [46], as shown in Figure 12.

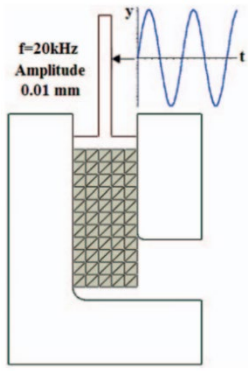

Figure 12. Applying ultrasonic vibration onto the plunger during the ECAP process reprinted with permission from Ref. [46]. Copyright 2022, ELSEVIER.

It was found that, when the plunger had ultrasound with a vibration amplitude of 2.5 μm at 20 kHz, much finer grains were achieved in the pure aluminum rods (as shown in Figure 13), and the calculated grain refinement efficiency of this improved the ECAP process increased by almost 25.8% [47].

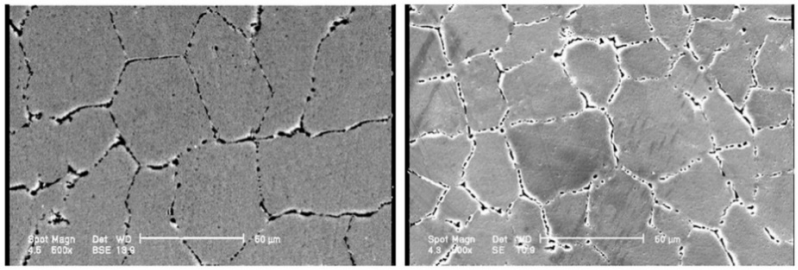

Figure 13. Microstructures of the conventional (left) and ultrasonic (right) ECAP-processed pure Al reprinted with permission from Ref. [47]. Copyright 2022, ELSEVIER.

2.2.3. Accumulative Roll Bonding (ARB)

Accumulative roll bonding (ARB) was first proposed in 1999 by Y. Sato et al. [48]. Compared with other bulk grain refinement methods, such as ECAP and HPT, which require large load capacities and many dies, its unique advantage is that it can be mass-produced at a lower operating cost, which makes it applicable to industrial manufacture. Its basic process is shown in Figure 14; in this process, the stacking of materials and traditional seam welding are repeated. Firstly, place one strip aligned on top of the other, clean the mating surfaces to remove layers of sediment, and then apply a wire brush to enhance the bonding strength between the materials [49]. The two layers are joined together by rolling, just as in a traditional rolling bonding process; then, the rolled material is cut in half. The cut strip is once again surface treated, stacked, and seam welded, and the whole process is repeated. The whole process should be conducted at an elevated temperature, but below recrystallization temperature because recrystallization will cancel out the accumulated strain. Low temperature would result in insufficient ductility and bond strength [48].

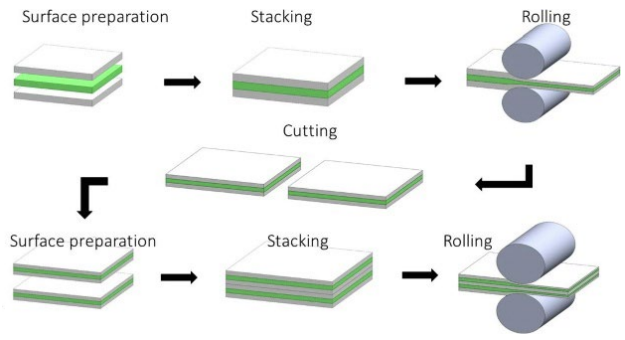

Figure 14. Diagrammatic representation of the accumulative roll-bonding (ARB) process reprinted with permission from Ref. [49]. Copyright 2022, ELSEVIER.

Ye et al. [50] used Ni, Ti, Al, and Cu as experimental objects and studied their microstructure evolution and mechanical properties during the ARB process. As revealed in Figure 15, with the increasing number of ARB passes, the thickness of the layers decreased gradually. It was reported that grain sizes decreased significantly with rolling reduction, and the grains in the layers near the surface possessed smaller grain sizes [51]. Furthermore, the corrosion resistance of the treated sample increased even when processed in the lower cycles [52]. Multi-layer composite metal materials can also be prepared using this method [53]. The shortcoming of ARB is that the process requires high precision and a long time; in addition, the quality of the final product is usually affected by the adhesion of the interlayers.

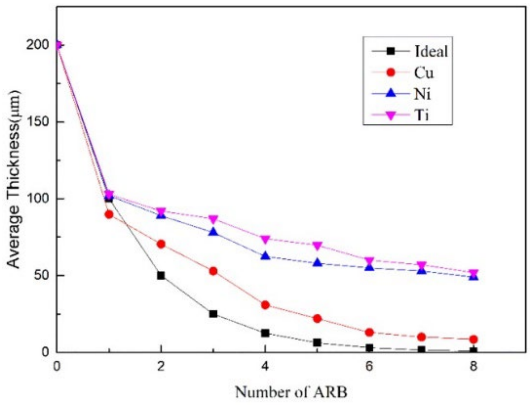

Figure 15. Variations of layer thickness versus the number of ARB passes reprinted with permission from Ref. [50]. Copyright 2022, ELSEVIER.

2.2.4. Hydrostatic Extrusion (HE)

The HE method was first proposed in the 1960s to improve the cold workability of brittle materials. Figure 16 shows a schematic diagram of the structure of the hydrostatic extrusion; the billet is packed into a container which is sealed and filled with pressure medium by a plunger, and then the sample is pressed/forced through the die when high pressure is supplied [54]. To ensure the tightness of the pressure chamber, special high-pressure seals are provided between the die and container as well as between the ram and container [55]. Since there is no metallic contact between the ram/vessel and the billet, and the uniform pressure can be applied to the product through the medium (such as castor oil), this method is optimal for fabricating products with complex shapes [54]. Compared with other SPD methods, one drawback of HE is that it can reduce the diameter of the product to avoid causing extremely high plastic deformation during the process. In addition, the limitations of HE include energy loss during compaction of the liquid medium, stringent requirements on the sealing structure, the need for fluid injection and fluid removal in each extrusion cycle, and some further complications that arise when it is performed at higher temperatures [56].

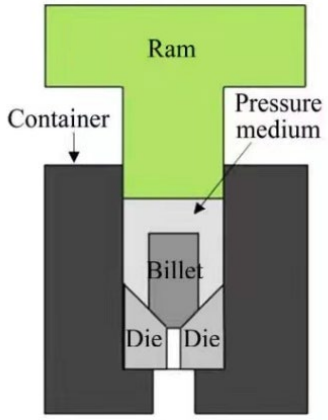

Figure 16. Schematic diagrams of hydrostatic extrusion reprinted with permission from Ref. [54]. Copyright 2022, ELSEVIER.

2.2.5. Multi-Directional Forging (MDF)

Multi-directional forging is a plastic deformation process that was proposed in the mid-1990s for the preparation of bulk ultrafine-grained metal materials. Its working principle is that the direction of the applied force is continuously changing during operation, and the multiple forgings in different directions of the billet are equivalent (as shown in Figures 17 and 18). Since its operating temperature is usually in the recrystallization

temperature range of the alloy and the load is relatively low, the MDF process can be used to prepare nanostructured/ultrafine-grained materials. During the MDF process, the change of the loading direction has a great influence on the rheological behavior and microstructure evolution of the material. With the applied pressure on the material in three vertical directions changing continuously, the relationship between flow stress and strain as well as the evolution process of the microstructure of the materials can be systematically studied [57]. The advantage of this method is that nanostructures can be obtained in rather brittle materials, since the process starts at high temperatures and the specific loads applied to the product are relatively low.

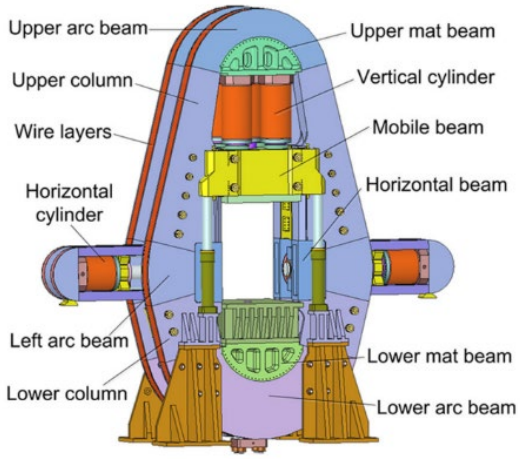

Figure 17. The main structure of MDF reprinted with permission from Ref. [58]. Copyright 2022, ELSEVIER.

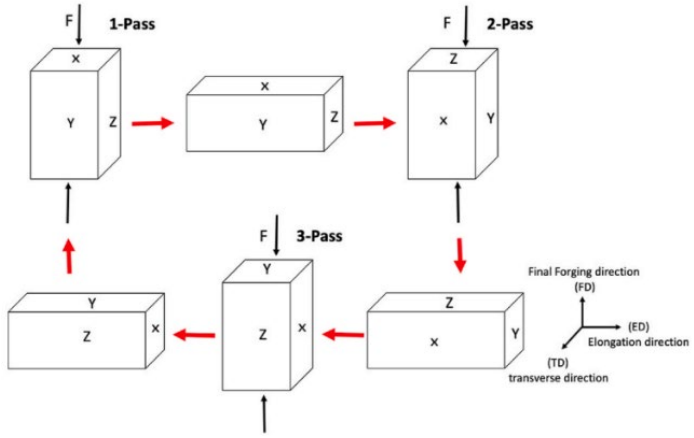

Figure 18. Process of MDF reprinted with permission from Ref. [59]. Copyright 2022, ELSEVIER.

3. Grain Refinement of Different Metallic Materials to Modulate Cell Response

The response of cells to biomaterials is very important, as it directly affects the osseointegration of the biomaterials after implantation and ultimately determines the success ratio of implantation surgery and the service life of the implants. Since the human bone matrix is mainly composed of nanoscale collagen and HA particles, surface/bulk nanostructuring metallic materials to mimic the nanostructure of the bone is obviously conducive to enhancing cellular responses. Cell behaviors such as adhesion, proliferation, differentiation, and mineralization on the various surface/bulk grain-refined metals are summarized below.

3.1. Titanium and Its Alloys

Titanium is the ninth most abundant element on earth, and its main source is rutile ore [60]. Titanium and its alloys have been widely used as implant materials because of

their excellent corrosion resistance, mechanical properties, and biocompatibility. Compared with coarse-grained counterparts, fine-grained titanium materials have been reported to exhibit better toughness, hardness, wear resistance, fatigue strength, etc. [61–63]. Cell responses to surface and bulk grain-refined titanium-based substrates are listed in Tables 1 and 2, respectively.

Table 1. Cell response to titanium and its alloys after surface grain refinement.

Material	Process	Grain Size	Cell Type	Cellular Behavior	Ref.
Ti-Nb alloy	SMAT, 5 min, 20 kHz	<100 nm	hMSC	Adhesion is enhanced	[61]
CpTi	USSP, 30–120 s, 20 kHz	20.23–23.80 nm	hMSC	Viability and proliferation are enhanced	[14]
CpTi (Grade 2)	SMAT, 30 min, 25 Hz	40 ± 15 nm	hMSC	Adhesion and proliferation are enhanced	[15]
CpTi plates	Ultrasonic-assisted SMAT, 20 min, 20 kHz	~56 nm	hMSC	Adhesion, proliferation, and osteogenic differentiation are enhanced	[17]
TLM alloy (Ti-25Nb-3Mo-2Sn3Zr)	SMAT, 30 min, 50 Hz	30–40 nm	Rabbit bone marrow mesenchymal stem cell	Adhesion, proliferation, osteogenic differentiation, and mineralization are enhanced	[64]
TLM alloy	SMAT, 60 min, 50 Hz	26 ± 5 nm	hFOB1.19	Adhesion, proliferation, osteogenic differentiation, and mineralization are enhanced	[65]
TLM alloy	SMAT, 20 kHz	29.7 nm	Osteoblastic cell	Adhesion, spreading, viability, and osteogenic differentiation are enhanced	[66]
TNTZ alloy (Ti-29Nb-13Ta-4.6Zr)	UNSM, 20 kHz	40–200 nm	Murine pre-osteoblast (MC3T3 cell)	Adhesion, spreading, and proliferation are enhanced	[62]
Pure Ti	USSP, 30 min, 50 kHz	57–88 nm	Human osteoblast-like cell (MG63)	Adhesion, proliferation, ALP activity, and calcium deposition are enhanced	[67]
CpTi	SMAT, 60 min	10 nm	Osteoblast cell (MG63 cell)	Adhesion, proliferation, and osteogenic differentiation are enhanced	[68]
CpTi	Ultrasonic-assisted SMAT, 20 min, 20 kHz	<100 nm	MG63 cell	Enhanced cell adhesion and proliferation, and alleviated cell apoptosis	[69]
CpTi	SMAT, 50 Hz	25.2 nm	Saos-2 cell	Enhanced adhesion and viability, and promotion of the progression of cells into the S phase	[70]

Table 2. Cell response to titanium and its alloys after bulk grain refinement.

Material	Process	Grain Size	Cell Type	Cellular Behavior	Ref.
CpTi (Grade 2 and Grade 4)	ECAP, pressing at 300 °C with a 90° angle channel	230 nm	Primary human adipose-derived mesenchymal stem cell	Mineralization and viability are enhanced	[71]
CpTi (Grade 2)	ECAP, pressing at 350 °C with a 90° angle channel, 8 passes	170–200 nm	hMSC	Adhesion and spreading are enhanced	[72]
CpTi (Grade 2)	ECAP, pressing at 400 °C with a 120° angle channel, 3 passes	500–700 nm	Human fetal osteoblast cell (hFOB1.19)	Adhesion, spreading, and viability are enhanced	[16]
CpTi (Grade 2)	MDF	<100 nm	MC3T3-E1 cell	Proliferation is enhanced	[73]
Ti-31.5Nb-3.1Zr-3.1Ta-0.9Fe-0.16O alloy	HPT, 1–2 GPa, 100–2000 rpm	<1000 nm	MC3T3-E1 cell	Adhesion, proliferation, and osteogenic differentiation are enhanced	[74]
TNTZ alloy	HPT	285 nm × 35 nm α needle and 12 nm β particle	Human osteoblast cell (hOB)	Attachment and proliferation are enhanced	[75]
CpTi	HPT, 6 GPa	10–50 nm	MC3T3-E1 cell	Attachment and spreading are enhanced	[76]
CpTi (Grade 2)	ECAP (pressing at 450 °C with a 90° angle channel, 4 passes) + SMAT (2 h, 6 Hz)	~420 nm	Homo sapiens human osteosarcoma cell (G292 cell)	Attachment, viability, and ALP activity are enhanced	[77]
CpTi (Grade 2 and Grade 4)	ECAP, pressing at 300 °C with a 90° angle channel	230 nm	Human osteosarcoma cell (Saos-2 cell)	Viability is enhanced	[71]
CpTi (Grade 2)	HE, 10 stages	87 nm	Saos-2 cell	Adhesion and proliferation are enhanced	[78]
CpTi (Grade 2)	ECAP, Route B_c	0.238 ± 0.05 μm	Mouse fibroblast cell	Adhesion and proliferation are enhanced	[79]
CpTi (Grade 2)	HE, 4 stages	~0.60 μm	Human umbilical vein endothelial cell (HUVEC)	(101(__)0) crystallographic plane favors cell attachment	[80]

3.2. Stainless Steel

Stainless steel is one of the most commonly used implant materials because of its low cost, good biocompatibility, and mechanical properties [81]. Medical stainless steel (mainly austenitic and martensitic) possessing low biological toxicity [82], representing a large category of medical metal materials, is widely used in human bone replacement, dentistry, cardiac surgery, coronary stent placement, and other fields. The common failures of medical stainless steel in a body fluid environment are largely caused by local corrosion (such as pitting, crevice, fatigue, and stress corrosion); in view of this, grain refinement has been

reported to be capable of enhancing its corrosion resistance effectively [83]. Cell responses to surface and bulk grain-refined stainless steel are listed in Tables 3 and 4, respectively.

Table 3. Cell response to stainless steel after surface grain refinement.

Material	Process	Grain Size	Cell Type	Cellular Behavior	Ref.
316L stainless steel	FSP, 1800 rpm	0.9 μm	Primary human dermal fibroblast	Spreading and proliferation are enhanced	[84]
316L stainless steel	FSP, 388 rpm	0.6 μm	Primary human dermal fibroblast	Viability is decreased	[85]
316L stainless steel	FSP, 1800 rpm	0.8 μm	MDCK-1 cell and HepG2	Enhanced cell attachment and proliferation, and restrained platelet and fibrinogen adhesion	[24]
316L stainless steel	SMAT, 50 Hz, 15 min	<50 nm	MC3T3-E1 cell	Viability and spreading are enhanced	[86]

Table 4. Cell response to stainless steel after bulk grain refinement.

Material	Process	Grain Size	Cell Type	Cellular Behavior	Ref.
316L stainless steel	Rolling, several passes	<1000 nm	Mouse fibroblast cell	Adhesion, viability, and proliferation are enhanced	[87]
316L stainless steel	Rolling, several passes	<1000 nm	MC3T3-E1 cell	Enhanced vinculin signals and actin stress fibers in the outer region of the cells	[88]
Austenitic stainless steel	MDF	200–400 nm	Pre-osteoblast cell	Adhesion and growth are enhanced	[89]
316L stainless steel	ECAP, pressing at 400 °C with a 120° angle channel, 8 passes	176 ± 10 nm	Multipotent mesenchymal stromal/stem cell (MMSC)	Enhanced cell proliferation and suppressed cell apoptosis	[90]

From Tables 1–4, we can deduce that surface grain refinement is capable of fabricating surface layers on titanium and stainless metals with a grain size that is usually in the nanometer regime (<100 nm), whereas bulk grain refinement normally refines the grains of these two kinds of biometals into the ultrafine-grained regime (100~1000 nm). Although with different grain-size scales, the surface and bulk grain-refined titanium and stainless metals both promote the viability, spread, and proliferation of fibroblasts (such as the L-929 and HGF cell lines); enhance the adhesion, proliferation, osteogenic differentiation, and mineralization of osteoblastic cells (including the hFOB1.19, MC3T3, MG63, and Saos-2 cell lines); and promote the differentiation of mesenchymal/stromal stem cells into osteoblasts. Since the interaction of the three types of cells (fibroblasts, osteoblasts and stem cells) with biometals is critical for successful osseointegration after implantation, the information shown in the Tables would be helpful for researchers in selecting the appropriate means to improve the clinical performance of implanted metallic materials.

3.3. Magnesium and Its Alloys

Magnesium-based metals were first introduced as orthopedic implant materials in the first half of the last century, when Lambotte used pure magnesium steel plates and gold-plated steel nails to fix calf fractures in 1907. Magnesium has a lower density and elastic modulus, and the modulus is very close to human's bone [91]. Furthermore, magnesium has excellent biocompatibility and degradability—properties which are difficult to acquire from other metallic materials. Although the main drawbacks in the practical usage of magnesium in the field of biomedicine are low strength and relatively rapid corrosion rate [35], grain-refined magnesium alloys have been found to have better mechanical properties and corrosion resistance [92,93]. Cell responses to surface/bulk grain-refined magnesium-based metals are summarized in Table 5.

Table 5. Cell response to magnesium and its alloys after surface/bulk grain refinement.

Material	Process	Grain Size	Cell Type	Cellular Behavior	Ref.
Mg-3Zn alloy	Rolling, 10 passes	<40 μm	MG63	Viability is decreased	[94]
AZ31B Mg alloy	UNSM, 20 kHz	<(40–100) μm	Adipose-derived stem cell (ADSC)	Adhesion is not compromised	[95]
ZM21 Mg alloy	ECAP, pressing at 220 °C with a 90° angle channel, 4 passes	~5.4 μm	MG63 cell	Viability is not compromised	[96]

3.4. NiTi Shape Memory Alloys

NiTi alloys are smart materials which possess the unique properties of shape memory effect and super elasticity [97]; as such, they have been widely used in biomedical applications, including in dentistry, orthopedics, and interventional therapy. Surface/bulk grain refinement was adopted for this kind of alloy to improve its corrosion resistance and biocompatibility [98,99]. Cell responses to surface/bulk grain-refined NiTi shape memory alloys are summarized Table 6.

Table 6. Cell response to NiTi shape memory alloys after surface/bulk grain refinement.

Material	Process	Grain Size	Cell Type	Cellular Behavior	Ref.
$Ni_{50.8}Ti_{49.2}$ alloy	ECAP, 8 passes	150–250 nm	Murine fibroblast cell line (L-929)	Viability, adhesion, proliferation, ALP activity, and mineralization are promoted	[97]
$Ni_{50.3}Ti_{49.7}$ alloy	LSP, laser with a wavelength of 1064 nm and intensity of 4 GW/cm^2	<1000 nm	Adipose-derived stem cell (ADSC)	Viability, growth, and spread are enhanced	[98]
$Ni_{50.8}Ti_{49.2}$ alloy	ECAP	200–300 nm	MG63 cell	Attachment and proliferation are boosted	[99]

3.5. Other Metals

Other metallic materials which are also frequently used as implant materials include tantalum, zirconium, etc. The effects of grain refinement of these metals on cell response are summarized in Table 7.

Table 7. Cell response after surface/bulk grain refinement.

Material	Process	Grain Size	Cell Type	Cellular Behavior	Ref.
Pure Zr	Rolling, 1 pass	~240 nm	Saos-2 cell and hMSC	Attachment, spreading, viability of Saos-2 cells, and ALP activity, mineralization nodule formation of hMSC are all unchanged	[100]
Nb-1Zr alloy	Accumulative Roll Bonding, 5 cycles	~800 nm	Mouse fibroblast (L-929), primary gingival fibroblast (HGF), and human osteoblast-like cell (U-2 OS)	Survival is not compromised	[101]
Pure Ta	Sliding Friction Treatment, 100 cycle	≤20 nm	hFOB1.19	Adhesion, proliferation, osteogenic differentiation, and maturation are enhanced	[102]

4. Discussion

SPD-induced surface and bulk grain refinement have been demonstrated in the above experiments as effective ways to improve cell response to biometals. However, grain-refined magnesium-based alloys exhibit comparable or even decreased cytocompatibility compared to coarse counterparts. As proposed by Nayak et al., grain size reduction could lead to accelerated corrosion of the magnesium alloy, release of H_2, and alteration of pH, constituting possible reasons for the discomfort of seeded cells [94]. For stainless steel, titanium, and NiTi alloys, studies on the surface and bulk grain refinement of these metals all affirm an effect on the enhancement of different cellular adhesion and functional expressions. Since bulk grain-refined metals usually undergo a mechanical polishing process before the seeding of cells, the enhanced cell response to the metals subjected to bulk grain

refinement can be mainly ascribed to three aspects: First, as proposed by Estrin et al. [72], when the grain size of the metals is decreased to the micro/nano regime, there will be a greater number of and more densely spaced nanopeaks as well as focal sites on the surface, facilitating cell adhesion and functions. Second, grain size reduction in metals usually leads to an increase in surface energy and an improvement in surface wettability [71,79,89]. Kiran et al. [16] reported that osteogenic cells tend to adhere and migrate on hydrophilic surfaces (high surface energy) rather than hydrophobic materials. Sun et al. [68] also believed that cells tend to adhere on material surfaces which display excellent wettability. In addition, it has also been proven that superior surface wettability can cause much larger lamellipodia structures along with a remarkably higher number of filopodia protrusions around the cells, thereby promoting the attachment and spreading of cells [75] as well as obliging the cells to extend their actin and myosin cytoskeletal fibers to reduce interfacial reactions [103]. Most importantly, grain refinement-induced better wettability can improve the protein adsorption capacity of treated biometals [65,69,70,104]. As is known, when a biometal is implanted into the body, it will soon absorb a large amount of proteins onto its surface, and through this adsorbed protein layer, cells interact with the biometal [105]. In other words, biomaterials regulate cells indirectly through their adsorbed proteins rather than their own direct signal [106]. Previously, it was reported that HPT-processed nano-grained titanium exhibited much better surface wettability compared to untreated titanium, displaying an obvious increase in absorption of fibronectin (a key protein involved in cell attachment, growth, and diffusion) on its surface, thereby greatly improving the cell attachment of pre-osteoblast cells [76]. As shown in Figure 19, after severe plastic deformation, an SPD-derived nano-grained surface has a higher proportion of grain boundaries and a larger number of small grooves and nanopeaks; these characteristics are conducive to increasing surface wettability and providing more adsorption and adhesion sites for the adsorption of proteins, consequently promoting cell adhesion and subsequent functional expression.

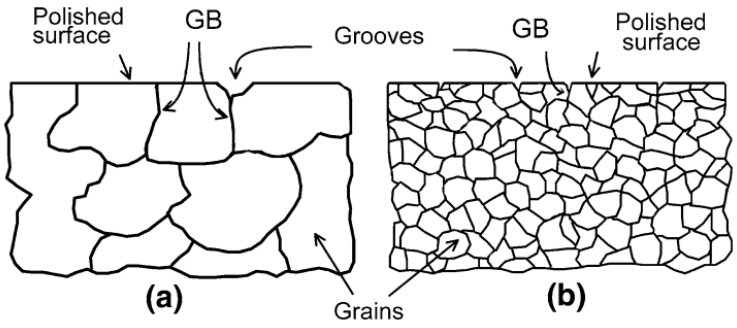

Figure 19. Schematic illustration of the presence of grooves on polished (**a**) coarse-grained and (**b**) nano-grained surfaces reprinted with permission from Ref. [79]. Copyright 2022, Springer.

Third, some studies [86,107] have noticed that the SPD process can generate an oxide layer of a certain thickness on the treated biometals, or change the physicochemical properties of its original oxide layer [78]. The surface oxide layer has been proven to be capable of improving hydrophilicity [76], and the related changes in physicochemical and electronic properties were found to be able to modulate protein adsorption [15,86]. Wang et al. [17] used the SPD method to treat titanium samples and obtained a gradient nanostructured surface (GNS) structure; the grain size of the material gradually increased from the surface to the inside, as shown in Figure 20. The authors inferred that the oxide layer formed on the GNS sample was much thicker and the ionic bond was more polar, which caused the adsorbed water on its surface to produce more hydroxyl groups, benefiting cell behavior [108]. Some studies have even pointed out that the formed thick and uniform oxide layer on an SPD-derived surface could enhance the binding of calcium ions and phosphate, and promote the effective adsorption of proteins from the biological medium, ultimately boosting cell proliferation and differentiation [109–112].

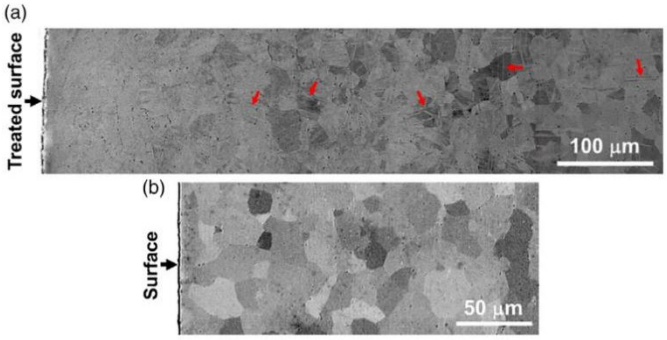

Figure 20. Cross-sectional scanning electron microscope (SEM) images of (**a**) gradient nanostructured surface (GNS) Ti samples and (**b**) coarse-grained (CG) Ti samples reprinted with permission from Ref. [17]. Copyright 2022, WILEY.

As for metals subjected to surface grain refinement, besides the above-mentioned factors, another reason accounting for the enhanced cell response is the SPD-generated surface roughness. Surface grain refinement causes obvious processing marks on the metal's surface, as reported in [14,16,80,113]. Greater surface roughness increases the surface area of biometals, thereby providing a larger contact region or bonding site for the cells to adhere to and ultimately influencing subsequent cell functions.

5. Conclusions

This review represents an attempt to summarize the methods of grain refinement and its effects on cell response to metallic materials commonly used in clinics. Recent studies have focused on alkali/acid etching, SPD, sol-gel, hydrothermal growth, thermal spraying, and electrochemical deposition methods, etc., to improve cell–material interactions for biometals. Among these methods, grain refinement achieved by the SPD process stands out for its unique advantage of escaping from the substrate-coating bonding issue. Surface and bulk grain refinement have been successfully realized for many biometals, such as titanium, stainless steel, magnesium, zirconium, tantalum, and their alloys as well as NiTi shape memory alloys. In general, these processes have exhibited positive effects on cell adhesion and subsequent functions, including proliferation; osteogenic differentiation; migration; and mineralization of different cellular types such as fibroblasts, osteoblasts, and stem cells during the culture time (from several hours to 21 days). The mechanism is related to the alteration of the surface nanotopography and the oxide layer state as well as the increase in surface energy, wettability, and protein adsorption capability. Nonetheless, more studies are needed to further characterize the relationship between process parameters and the grain scale of different biometals, and to disclose the critical grain size after SPD which could effectively influence cell response. Furthermore, surface/bulk grain refined metals should be implanted into different animal models to ensure their future use in clinics.

Author Contributions: Conceptualization, Y.G., R.H. and Y.H.; methodology, Y.G., R.H. and Y.H.; validation, Y.G., R.H. and Y.H.; formal analysis, Y.G., R.H. and Y.H.; investigation, Y.G., R.H. and Y.H.; resources, Y.G., R.H. and Y.H.; data curation, Y.G., R.H. and Y.H.; writing—original draft preparation, Y.G., R.H. and Y.H.; writing—review and editing, Y.G., R.H. and Y.H.; visualization, Y.G., R.H. and Y.H.; supervision, Y.G., R.H. and Y.H.; project administration, Y.G., R.H. and Y.H.; funding acquisition, R.H. All authors have read and agreed to the published version of the manuscript.

Funding: This research was funded by the Natural Science Research Projects of Anhui Universities, grant numbers KJ2020A0304 and KJ2019A0127, and the Research Foundation of the Institute of Environment-friendly Materials and Occupational Health of Anhui University of Science and Technology (Wuhu), grant number ALW2021YF07.

Data Availability Statement: Not applicable.

Conflicts of Interest: The authors declare no conflict of interest. The authors would like to disclose the following relationships: Y.G. and Y.H. are two masters of Anhui University of Science and Technology, and R.H.is the supervisor of these two masters. None of the above relationships has influenced the representation or interpretation of reported data or the collection, analysis, and interpretation thereof.

References

1. Misra, S.; Raghuwanshi, S. Enhancing the mechanical and biological performance of a metallic biomaterial for orthopedic applications. In *Fundamental Biomaterials: Metals*; Woodhead Publishing: Duxford, UK, 2018; pp. 355–370.
2. Kaur, G.; Kumar, V.; Baino, F.; Mauro, J.C.; Pickrell, G.; Evans, I.; Bretcanu, O. Mechanical properties of bioactive glasses, ceramics, glass-ceramics and composites: State-of-the-art review and future challenges. *Mater. Sci. Eng. C Mater. Biol. Appl.* **2019**, *104*, 109895. [CrossRef] [PubMed]
3. Williams, D.F. On the mechanisms of biocompatibility. *Biomaterials* **2008**, *29*, 2941–2953. [CrossRef] [PubMed]
4. Kuo, T.-Y.; Chin, W.-H.; Chien, C.-S.; Hsieh, Y.-H. Mechanical and biological properties of graded porous tantalum coatings deposited on titanium alloy implants by vacuum plasma spraying. *Surf. Coat. Technol.* **2019**, *372*, 399–409. [CrossRef]
5. Lo, Y.S.; Chang, C.C.; Lin, P.C.; Lin, S.P.; Wang, C.L. Direct growth of structurally controllable hydroxyapatite coating on Ti-6Al-4V through a rapid hydrothermal synthesis. *Appl. Surf. Sci.* **2021**, *556*, 149672. [CrossRef]
6. Lv, Y.; Sun, S.; Zhang, X.; Lu, X.; Dong, Z. Construction of multi-layered Zn-modified TiO2 coating by ultrasound-auxiliary micro-arc oxidation: Microstructure and biological property. *Mater. Sci. Eng. C Mater. Biol. Appl.* **2021**, *131*, 112487. [CrossRef] [PubMed]
7. Estrin, Y.; Kim, H.E.; Lapovok, R.; Ng, H.P.; Jo, J.H. Mechanical strength and biocompatibility of ultrafine-grained commercial purity titanium. *Biomed. Res. Int.* **2013**, *2013*, 914764. [CrossRef]
8. Parfenov, E.V.; Parfenova, L.V.; Dyakonov, G.S.; Danilko, K.V.; Mukaeva, V.R.; Farrakhov, R.G.; Lukina, E.S.; Valiev, R.Z. Surface functionalization via PEO coating and RGD peptide for nanostructured titanium implants and their in vitro assessment. *Surf. Coat. Technol.* **2019**, *357*, 669–683. [CrossRef]
9. Zheng, C.Y.; Nie, F.L.; Zheng, Y.F.; Cheng, Y.; Wei, S.C.; Valiev, R.Z. Enhanced in vitro biocompatibility of ultrafine-grained titanium with hierarchical porous surface. *Appl. Surf. Sci.* **2011**, *257*, 5634–5640. [CrossRef]
10. Edalati, K.; Bachmaier, A.; Beloshenko, V.A.; Beygelzimer, Y.; Blank, V.D.; Botta, W.J.; Bryła, K.; Čížek, J.; Divinski, S.; Enikeev, N.A.; et al. Nanomaterials by severe plastic deformation: Review of historical developments and recent advances. *Mater. Res. Lett.* **2022**, *10*, 163–256. [CrossRef]
11. Kalantari, K.; Saleh, B.; Webster, T.J. Biological Applications of Severely Plastically Deformed Nano-Grained Medical Devices: A Review. *Nanomaterials* **2021**, *11*, 748. [CrossRef]
12. Dobatkin, S.; Martynenko, N.; Anisimova, N.; Kiselevskiy, M.; Prosvirnin, D.; Terentiev, V.; Yurchenko, N.; Salishchev, G.; Estrin, Y. Mechanical Properties, Biodegradation, and Biocompatibility of Ultrafine Grained Magnesium Alloy WE43. *Materials* **2019**, *12*, 3627. [CrossRef] [PubMed]
13. Lu, K.; Lu, J. Nanostructured surface layer on metallic materials induced by surface mechanical attrition treatment. *Mater. Sci. Eng. A* **2004**, *375–377*, 38–45. [CrossRef]
14. Agrawal, R.K.; Pandey, V.; Barhanpurkar-Naik, A.; Wani, M.R.; Chattopadhyay, K.; Singh, V. Effect of ultrasonic shot peening duration on microstructure, corrosion behavior and cell response of cp-Ti. *Ultrasonics* **2020**, *104*, 106110. [CrossRef] [PubMed]
15. Bahl, S.; Aleti, B.T.; Suwas, S.; Chatterjee, K. Surface nanostructuring of titanium imparts multifunctional properties for orthopedic and cardiovascular applications. *Mater. Des.* **2018**, *144*, 169–181. [CrossRef]
16. Sandeep Kranthi Kiran, A.; Sireesha, M.; Ramalingam, R.; Kizhakeyil, A.; Verma, N.K.; Lakshminarayanan, R.; Sampath Kumar, T.S.; Doble, M.; Ramakrishna, S. Modulation of biological properties by grain refinement and surface modification on titanium surfaces for implant-related infections. *J. Mater. Sci.* **2019**, *54*, 13265–13282. [CrossRef]
17. Wang, W.; Wang, Z.; Fu, Y.; Dunne, N.; Liang, C.; Luo, X.; Liu, K.; Li, X.; Pang, X.; Lu, K. Improved osteogenic differentiation of human amniotic mesenchymal stem cells on gradient nanostructured Ti surface. *J. Biomed. Mater. Res. A* **2020**, *108*, 1824–1833. [CrossRef]
18. Tao, N.R.; Lu, J.; Lu, K. Surface Nanocrystallization by Surface Mechanical Attrition Treatment. *Mater. Sci. Forum* **2008**, *579*, 91–108. [CrossRef]
19. Tao, N.R.; Wang, Z.B.; Tong, W.P.; Sui, M.L.; Lu, J.; Lu, K. An investigation of surface nanocrystallization mechanism in Fe induced by surface mechanical attrition treatment. *Acta Mater.* **2002**, *50*, 4603–4616. [CrossRef]
20. Tao, N.R.; Sui, M.L.; Lu, J.; Lu, K. Surface nanocrystallization of iron induced by ultrasonic shot peening. *Nanostructured Mater.* **1999**, *11*, 433–440. [CrossRef]
21. Chaise, T.; Li, J.; Nélias, D.; Kubler, R.; Taheri, S.; Douchet, G.; Robin, V.; Gilles, P. Modelling of multiple impacts for the prediction of distortions and residual stresses induced by ultrasonic shot peening (USP). *J. Mater. Processing Technol.* **2012**, *212*, 2080–2090. [CrossRef]
22. Dhakal, B.; Swaroop, S. Review: Laser shock peening as post welding treatment technique. *J. Manuf. Processes* **2018**, *32*, 721–733. [CrossRef]
23. Acharya, S.; Suwas, S.; Chatterjee, K. Review of recent developments in surface nanocrystallization of metallic biomaterials. *Nanoscale* **2021**, *13*, 2286–2301. [CrossRef] [PubMed]

24. Perumal, G.; Ayyagari, A.; Chakrabarti, A.; Kannan, D.; Pati, S.; Grewal, H.S.; Mukherjee, S.; Singh, S.; Arora, H.S. Friction Stir Processing of Stainless Steel for Ascertaining Its Superlative Performance in Bioimplant Applications. *ACS Appl. Mater. Interfaces* **2017**, *9*, 36615–36631. [CrossRef] [PubMed]
25. Węglowski, M.S. Friction stir processing—State of the art. *Arch. Civ. Mech. Eng.* **2018**, *18*, 114–129. [CrossRef]
26. Merah, N.; Abdul Azeem, M.; Abubaker, H.M.; Al-Badour, F.; Albinmousa, J.; Sorour, A.A. Friction Stir Processing Influence on Microstructure, Mechanical, and Corrosion Behavior of Steels: A Review. *Materials* **2021**, *14*, 5023. [CrossRef]
27. Mironov, S.; Sato, Y.S.; Kokawa, H. Friction-stir processing. In *Nanocrystalline Titanium*; Elsevier: Amsterdam, The Netherlands, 2019; pp. 55–69.
28. Maleki, E.; Unal, O.; Guagliano, M.; Bagherifard, S. The effects of shot peening, laser shock peening and ultrasonic nanocrystal surface modification on the fatigue strength of Inconel 718. *Mater. Sci. Eng. Struct. Mater. Prop. Microstruct. Processing* **2021**, *810*, 141029. [CrossRef]
29. Liu, R.Y.; Yuan, S.; Lin, N.M.; Zeng, Q.F.; Wang, Z.H.; Wu, Y.C. Application of ultrasonic nanocrystal surface modification (UNSM) technique for surface strengthening of titanium and titanium alloys: A mini review. *J. Mater. Res. Technol. JmrT* **2021**, *11*, 351–377. [CrossRef]
30. Liang, Y.; Qin, H.F.; Mehra, N.; Zhu, J.H.; Yang, Z.N.; Doll, G.L.; Ye, C.; Dong, Y.L. Controllable hierarchical micro/nano patterns on biomaterial surfaces fabricated by ultrasonic nanocrystalline surface modification. *Mater. Des.* **2018**, *137*, 325–334. [CrossRef]
31. Amanov, A.; Cho, I.S.; Pyoun, Y.S.; Lee, C.S.; Park, I.G. Micro-dimpled surface by ultrasonic nanocrystal surface modification and its tribological effects. *Wear* **2012**, *286*, 136–144. [CrossRef]
32. Moon, J.H.; Baek, S.M.; Lee, S.G.; Seong, Y.; Amanov, A.; Lee, S.; Kim, H.S. Effects of residual stress on the mechanical properties of copper processed using ultrasonic-nanocrystalline surface modification. *Mater. Res. Lett.* **2018**, *7*, 97–102. [CrossRef]
33. Edalati, K.; Horita, Z. A review on high-pressure torsion (HPT) from 1935 to 1988. *Mater. Sci. Eng. A* **2016**, *652*, 325–352. [CrossRef]
34. Azushima, A.; Kopp, R.; Korhonen, A.; Yang, D.Y.; Micari, F.; Lahoti, G.D.; Groche, P.; Yanagimoto, J.; Tsuji, N.; Rosochowski, A.; et al. Severe plastic deformation (SPD) processes for metals. *Cirp Ann. Manuf. Technol.* **2008**, *57*, 716–735. [CrossRef]
35. Figueiredo, R.B.; Langdon, T.G. Processing Magnesium and Its Alloys by High-Pressure Torsion: An Overview. *Adv. Eng. Mater.* **2019**, *21*, 1801039. [CrossRef]
36. Faraji, G.; Kim, H.S.; Kashi, H.T. Severe Plastic Deformation Methods for Bulk Samples. In *Severe Plastic Deformation*; Elsevier: Amsterdam, The Netherlands, 2018; pp. 37–112.
37. Sadasivan, N.; Balasubramanian, M.; Rameshbapu, B.R. A comprehensive review on equal channel angular pressing of bulk metal and sheet metal process methodology and its varied applications. *J. Manuf. Processes* **2020**, *59*, 698–726. [CrossRef]
38. Yamashita, A.; Horita, Z.; Langdon, T.G. Improving the mechanical properties of magnesium and a magnesium alloy through severe plastic deformation. *Mater. Sci. Eng. A* **2001**, *300*, 142–147. [CrossRef]
39. Zhang, Q.; Li, Q.A.; Chen, X.Y. Research progress of ultrafine grained magnesium alloy prepared by equal channel angular pressing. *Mater. Res. Express* **2021**, *8*, 022001. [CrossRef]
40. Valiev, R.Z.; Islamgaliev, R.K.; Alexandrov, I.V. Bulk nanostructured materials from severe plastic deformation. *Prog. Mater. Sci.* **2000**, *45*, 103–189. [CrossRef]
41. Suo, T.; Li, Y.; Deng, Q.; Liu, Y. Optimal pressing route for continued equal channel angular pressing by finite element analysis. *Mater. Sci. Eng. A* **2007**, *466*, 166–171. [CrossRef]
42. Stolyarov, V.V.; Zhu, Y.T.; Alexandrov, I.V.; Lowe, T.C.; Valiev, R.Z. Influence of ECAP routes on the microstructure and properties of pure Ti. *Mater. Sci. Eng. A* **2001**, *299*, 59–67. [CrossRef]
43. Elias, C.N.; Meyers, M.A.; Valiev, R.Z.; Monteiro, S.N. Ultrafine grained titanium for biomedical applications: An overview of performance. *J. Mater. Res. Technol.* **2013**, *2*, 340–350. [CrossRef]
44. Mora-Sanchez, H.; Sabirov, I.; Monclus, M.A.; Matykina, E.; Molina-Aldareguia, J.M. Ultra-fine grained pure Titanium for biomedical applications. *Mater. Technol.* **2016**, *31*, 756–771. [CrossRef]
45. Verlinden, B. Severe plastic deformation of metals. *Metal. J. Metall.* **2005**, *11*, 165–182. [CrossRef]
46. Ahmadi, F.; Farzin, M. Finite element analysis of ultrasonic-assisted equal channel angular pressing. *Proc. Inst. Mech. Eng. Part C J. Mech. Eng. Sci.* **2013**, *228*, 1859–1868. [CrossRef]
47. Ahmadi, F.; Farzin, M.; Meratian, M.; Loeian, S.M.; Forouzan, M.R. Improvement of ECAP process by imposing ultrasonic vibrations. *Int. J. Adv. Manuf. Technol.* **2015**, *79*, 503–512. [CrossRef]
48. Saito, Y.; Utsunomiya, H.; Tsuji, N.; Sakai, T. Novel ultra-high straining process for bulk materials—development of the accumulative roll-bonding (ARB) process. *Acta Mater.* **1999**, *47*, 579–583. [CrossRef]
49. Rao, G.N.M.; Kumar, V.R.M. A review on recent advances in accumulative roll bonding of similar, dissimilar and metal matrix composites. *Mater. Today Proc.* **2021**, *56*, A13–A18. [CrossRef]
50. Ye, N.; Ren, X.; Liang, J. Microstructure and mechanical properties of Ni/Ti/Al/Cu composite produced by accumulative roll bonding (ARB) at room temperature. *J. Mater. Res. Technol.* **2020**, *9*, 5524–5532. [CrossRef]
51. McCabe, R.J.; Nizolek, T.J.; Li, N.; Zhang, Y.F.; Coughlin, D.R.; Miller, C.; Carpenter, J.S. Evolution of microstructures and properties leading to layer instabilities during accumulative roll bonding of Fe-Cu, Fe-Ag, and Fe-Al. *Mater. Des.* **2021**, *212*, 110204. [CrossRef]
52. Kadkhodaee, M.; Babaiee, M.; Manesh, H.D.; Pakshir, M.; Hashemi, B. Evaluation of corrosion properties of Al/nanosilica nanocomposite sheets produced by accumulative roll bonding (ARB) process. *J. Alloy. Compd.* **2013**, *576*, 66–71. [CrossRef]

53. Shakouri, S.; Eghbali, B. Characterization of Microstructure and Mechanical Properties of Multilayer Al/Cu/Mg/Ni Composite Produced through Accumulative Roll Bonding. *Phys. Met. Metallogr.* **2019**, *120*, 796–805. [CrossRef]
54. Lee, J.; Jeong, H.; Park, S. Effect of extrusion ratios on hardness, microstructure, and crystal texture anisotropy in pure niobium tubes subjected to hydrostatic extrusion. *Trans. Nonferrous Met. Soc. China* **2021**, *31*, 1689–1699. [CrossRef]
55. Sillekens, W.H.; Bohlen, J. Hydrostatic extrusion of magnesium alloys. In *Advances in Wrought Magnesium Alloys*; Woodhead Publishing: Duxford, UK, 2012; pp. 323–345.
56. Garbacz, H.; Topolski, K.; Motyka, M. Hydrostatic extrusion. In *Nanocrystalline Titanium*; Elsevier: Amsterdam, The Netherlands, 2019; pp. 37–53.
57. Sakai, T.; Belyakov, A.; Kaibyshev, R.; Miura, H.; Jonas, J.J. Dynamic and post-dynamic recrystallization under hot, cold and severe plastic deformation conditions. *Prog. Mater. Sci.* **2014**, *60*, 130–207. [CrossRef]
58. Wang, W.; Lin, F.; Zhang, L.; Wang, X. Experimental study and finite element analysis on the frame of multi-directional forging press. *Proc. Inst. Mech. Eng. Part B J. Eng. Manuf.* **2016**, *231*, 2112–2122. [CrossRef]
59. Shahriyari, F.; Shaeri, M.H.; Dashti, A.; Zarei, Z.; Noghani, M.T.; Cho, J.H.; Djavanroodi, F. Evolution of mechanical properties, microstructure and texture and of various brass alloys processed by multi-directional forging. *Mater. Sci. Eng. A* **2022**, *831*, 142149. [CrossRef]
60. Perks, C.; Mudd, G. Titanium, zirconium resources and production: A state of the art literature review. *Ore Geol. Rev.* **2019**, *107*, 629–646. [CrossRef]
61. Weiss, L.; Nessler, Y.; Novelli, M.; Laheurte, P.; Grosdidier, T. On the Use of Functionally Graded Materials to Differentiate the Effects of Surface Severe Plastic Deformation, Roughness and Chemical Composition on Cell Proliferation. *Metals* **2019**, *9*, 1344. [CrossRef]
62. Kheradmandfard, M.; Kashani-Bozorg, S.F.; Lee, J.S.; Kim, C.-L.; Hanzaki, A.Z.; Pyun, Y.-S.; Cho, S.-W.; Amanov, A.; Kim, D.-E. Significant improvement in cell adhesion and wear resistance of biomedical β-type titanium alloy through ultrasonic nanocrystal surface modification. *J. Alloy. Compd.* **2018**, *762*, 941–949. [CrossRef]
63. Valiev, R.Z.; Parfenov, E.V.; Parfenova, L.V. Developing Nanostructured Metals for Manufacturing of Medical Implants with Improved Design and Biofunctionality. *Mater. Trans.* **2019**, *60*, 1356–1366. [CrossRef]
64. Huang, R.; Liu, L.; Li, B.; Qin, L.; Huang, L.; Yeung, K.W.K.; Han, Y. Nanograins on Ti-25Nb-3Mo-2Sn-3Zr alloy facilitate fabricating biological surface through dual-ion implantation to concurrently modulate the osteogenic functions of mesenchymal stem cells and kill bacteria. *J. Mater. Sci. Technol.* **2021**, *73*, 31–44. [CrossRef]
65. Huang, R.; Zhang, L.; Huang, L.; Zhu, J. Enhanced in-vitro osteoblastic functions on beta-type titanium alloy using surface mechanical attrition treatment. *Mater. Sci. Eng. C Mater Biol. Appl.* **2019**, *97*, 688–697. [CrossRef]
66. Zhao, C.; Cao, P.; Ji, W.; Han, P.; Zhang, J.; Zhang, F.; Jiang, Y.; Zhang, X. Hierarchical titanium surface textures affect osteoblastic functions. *J. Biomed. Mater. Res. A* **2011**, *99*, 666–675. [CrossRef] [PubMed]
67. Guo, Y.; Hu, B.; Tang, C.; Wu, Y.; Sun, P.; Zhang, X.; Jia, Y. Increased osteoblast function in vitro and in vivo through surface nanostructuring by ultrasonic shot peening. *Int. J. Nanomed.* **2015**, *10*, 4593–4603. [CrossRef]
68. Sun, J.; Yao, Q.T.; Zhang, Y.H.; Du, X.D.; Wu, Y.C.; Tong, W.P. Simultaneously improving surface mechanical properties and in vitro biocompatibility of pure titanium via surface mechanical attrition treatment combined with low-temperature plasma nitriding. *Surf. Coat. Technol.* **2017**, *309*, 382–389. [CrossRef]
69. Luo, X.; Liang, C.; Li, N.; Zhu, Y.H.; Cao, N.J.; Wang, J.; Liu, K.D.; Zhao, H.W.; Wang, Z.B.; Wang, W. Effect of Gradient Nanostructured Ti on Behaviours of MG63 Cells In Vitro. *J. Nanomater.* **2020**, *2020*, 1–11. [CrossRef]
70. Zhao, C.; Han, P.; Ji, W.; Zhang, X. Enhanced mechanical properties and in vitro cell response of surface mechanical attrition treated pure titanium. *J. Biomater. Appl.* **2012**, *27*, 113–118. [CrossRef] [PubMed]
71. Medvedev, A.E.; Neumann, A.; Ng, H.P.; Lapovok, R.; Kasper, C.; Lowe, T.C.; Anumalasetty, V.N.; Estrin, Y. Combined effect of grain refinement and surface modification of pure titanium on the attachment of mesenchymal stem cells and osteoblast-like SaOS-2 cells. *Mater. Sci. Eng. C Mater. Biol. Appl.* **2017**, *71*, 483–497. [CrossRef] [PubMed]
72. Estrin, Y.; Ivanova, E.P.; Michalska, A.; Truong, V.K.; Lapovok, R.; Boyd, R. Accelerated stem cell attachment to ultrafine grained titanium. *Acta Biomater.* **2011**, *7*, 900–906. [CrossRef]
73. Ito, Y.; Hoshi, N.; Hayakawa, T.; Ohkubo, C.; Miura, H.; Kimoto, K. Mechanical properties and biological responses of ultrafine-grained pure titanium fabricated by multi-directional forging. *Mater. Sci. Eng. B* **2019**, *245*, 30–36. [CrossRef]
74. Gurau, C.; Gurau, G.; Mitran, V.; Dan, A.; Cimpean, A. The Influence of Severe Plastic Deformation on Microstructure and In Vitro Biocompatibility of the New Ti-Nb-Zr-Ta-Fe-O Alloy Composition. *Materials* **2020**, *13*, 4853. [CrossRef]
75. Yilmazer, H.; Şen, M.; Niinomi, M.; Nakai, M.; Huihong, L.; Cho, K.; Todaka, Y.; Shiku, H.; Matsue, T. Developing biomedical nano-grained β-type titanium alloys using high pressure torsion for improved cell adherence. *RSC Adv.* **2016**, *6*, 7426–7430. [CrossRef]
76. Faghihi, S.; Azari, F.; Zhilyaev, A.P.; Szpunar, J.A.; Vali, H.; Tabrizian, M. Cellular and molecular interactions between MC3T3-E1 pre-osteoblasts and nanostructured titanium produced by high-pressure torsion. *Biomaterials* **2007**, *28*, 3887–3895. [CrossRef]
77. Attarilar, S.; Salehi, M.T.; Al-Fadhalah, K.J.; Djavanroodi, F.; Mozafari, M. Functionally graded titanium implants: Characteristic enhancement induced by combined severe plastic deformation. *PLoS ONE* **2019**, *14*, e0221491. [CrossRef] [PubMed]
78. Kubacka, D.; Yamamoto, A.; Wieciński, P.; Garbacz, H. Biological behavior of titanium processed by severe plastic deformation. *Appl. Surf. Sci.* **2019**, *472*, 54–63. [CrossRef]

79. Kim, T.N.; Balakrishnan, A.; Lee, B.C.; Kim, W.S.; Dvorankova, B.; Smetana, K.; Park, J.K.; Panigrahi, B.B. In vitro fibroblast response to ultra fine grained titanium produced by a severe plastic deformation process. *J. Mater. Sci. Mater. Med.* **2008**, *19*, 553–557. [CrossRef] [PubMed]
80. Wojtas, D.; Mzyk, A.; Kawalko, J.; Imbir, G.; Trembecka-Wojciga, K.; Marzec, M.; Jarzebska, A.; Maj, L.; Wierzbanowski, K.; Chulist, R.; et al. Texture-Governed Cell Response to Severely Deformed Titanium. *ACS Biomater. Sci. Eng.* **2021**, *7*, 114–121. [CrossRef]
81. Bekmurzayeva, A.; Duncanson, W.J.; Azevedo, H.S.; Kanayeva, D. Surface modification of stainless steel for biomedical applications: Revisiting a century-old material. *Mater. Sci. Eng. C Mater. Biol. Appl.* **2018**, *93*, 1073–1089. [CrossRef]
82. Chen, Q.Z.; Thouas, G.A. Metallic implant biomaterials. *Mater. Sci. Eng. R-Rep.* **2015**, *87*, 1–57. [CrossRef]
83. Zhang, H.; Xue, P.; Wu, L.H.; Song, Q.N.; Wang, D.; Xiao, B.L.; Ma, Z.Y. Effect of grain ultra-refinement on corrosion behavior of ultra-high strength high nitrogen stainless steel. *Corros. Sci.* **2020**, *174*, 108847. [CrossRef]
84. Perumal, G.; Chakrabarti, A.; Grewal, H.S.; Pati, S.; Singh, S.; Arora, H.S. Enhanced antibacterial properties and the cellular response of stainless steel through friction stir processing. *Biofouling* **2019**, *35*, 187–203. [CrossRef]
85. Perumal, G.; Grewal, H.S.; Arora, H.S. Enhanced durability, bio-activity and corrosion resistance of stainless steel through severe surface deformation. *Colloids Surf. B Biointerfaces* **2020**, *194*, 111197. [CrossRef]
86. Bahl, S.; Shreyas, P.; Trishul, M.A.; Suwas, S.; Chatterjee, K. Enhancing the mechanical and biological performance of a metallic biomaterial for orthopedic applications through changes in the surface oxide layer by nanocrystalline surface modification. *Nanoscale* **2015**, *7*, 7704–7716. [CrossRef] [PubMed]
87. Misra, R.D.; Thein-Han, W.W.; Pesacreta, T.C.; Somani, M.C.; Karjalainen, L.P. Biological significance of nanograined/ultrafine-grained structures: Interaction with fibroblasts. *Acta Biomater.* **2010**, *6*, 3339–3348. [CrossRef] [PubMed]
88. Misra, R.D.; Thein-Han, W.W.; Pesacreta, T.C.; Hasenstein, K.H.; Somani, M.C.; Karjalainen, L.P. Cellular response of preosteoblasts to nanograined/ultrafine-grained structures. *Acta Biomater.* **2009**, *5*, 1455–1467. [CrossRef]
89. Gong, N.; Hu, C.; Hu, B.; An, B.; Misra, R.D.K. On the mechanical behavior of austenitic stainless steel with nano/ultrafine grains and comparison with micrometer austenitic grains counterpart and their biological functions. *J. Mech. Behav. Biomed. Mater.* **2020**, *101*, 103433. [CrossRef] [PubMed]
90. Rybalchenko, O.V.; Anisimova, N.Y.; Kiselevsky, M.V.; Belyakov, A.N.; Tokar, A.A.; Terent'ev, V.F.; Prosvirnin, D.V.; Rybalchenko, G.V.; Raab, G.I.; Dobatkin, S.V. The influence of ultrafine-grained structure on the mechanical properties and biocompatibility of austenitic stainless steels. *J. Biomed. Mater. Res. B Appl. Biomater.* **2020**, *108*, 1460–1468. [CrossRef] [PubMed]
91. Staiger, M.P.; Pietak, A.M.; Huadmai, J.; Dias, G. Magnesium and its alloys as orthopedic biomaterials: A review. *Biomaterials* **2006**, *27*, 1728–1734. [CrossRef]
92. Liao, H.B.; Mo, L.L.; Zhou, X.; Zhao, B.; Du, J. Grain refinement and improvement of mechanical properties of AZ31 magnesium alloy inoculated by in-situ oxidation process. *J. Mater. Res. Technol. JmrT* **2021**, *12*, 807–817. [CrossRef]
93. Patel, V.; Li, W.; Andersson, J.; Li, N. Enhancing grain refinement and corrosion behavior in AZ31B magnesium alloy via stationary shoulder friction stir processing. *J. Mater. Res. Technol.* **2022**, *17*, 3150–3156. [CrossRef]
94. Nayak, S.; Bhushan, B.; Jayaganthan, R.; Gopinath, P.; Agarwal, R.D.; Lahiri, D. Strengthening of Mg based alloy through grain refinement for orthopaedic application. *J. Mech. Behav. Biomed. Mater.* **2016**, *59*, 57–70. [CrossRef]
95. Hou, X.; Qin, H.; Gao, H.; Mankoci, S.; Zhang, R.; Zhou, X.; Ren, Z.; Doll, G.L.; Martini, A.; Sahai, N.; et al. A systematic study of mechanical properties, corrosion behavior and biocompatibility of AZ31B Mg alloy after ultrasonic nanocrystal surface modification. *Mater. Sci. Eng. C Mater. Biol. Appl.* **2017**, *78*, 1061–1071. [CrossRef]
96. Prithivirajan, S.; Nyahale, M.B.; Naik, G.M.; Narendranath, S.; Prabhu, A.; Rekha, P.D. Bio-corrosion impacts on mechanical integrity of ZM21 Mg for orthopaedic implant application processed by equal channel angular pressing. *J. Mater. Sci. Mater. Med.* **2021**, *32*, 65. [CrossRef] [PubMed]
97. Li, H.F.; Nie, F.L.; Zheng, Y.F.; Cheng, Y.; Wei, S.C.; Valiev, R.Z. Nanocrystalline Ti49.2Ni50.8 shape memory alloy as orthopaedic implant material with better performance. *J. Mater. Sci. Technol.* **2019**, *35*, 2156–2162. [CrossRef]
98. Zhang, R.; Mankoci, S.; Walters, N.; Gao, H.; Zhang, H.; Hou, X.; Qin, H.; Ren, Z.; Zhou, X.; Doll, G.L.; et al. Effects of laser shock peening on the corrosion behavior and biocompatibility of a nickel-titanium alloy. *J. Biomed. Mater. Res. B Appl. Biomater.* **2019**, *107*, 1854–1863. [CrossRef] [PubMed]
99. Zheng, C.Y.; Nie, F.L.; Zheng, Y.F.; Cheng, Y.; Wei, S.C.; Valiev, R.Z. Enhanced in vitro biocompatibility of ultrafine-grained biomedical NiTi alloy with microporous surface. *Appl. Surf. Sci.* **2011**, *257*, 9086–9093. [CrossRef]
100. Saldana, L.; Mendez-Vilas, A.; Jiang, L.; Multigner, M.; Gonzalez-Carrasco, J.L.; Perez-Prado, M.T.; Gonzalez-Martin, M.L.; Munuera, L.; Vilaboa, N. In vitro biocompatibility of an ultrafine grained zirconium. *Biomaterials* **2007**, *28*, 4343–4354. [CrossRef]
101. Rodríguez-Espinoza, B.L.; García-Pastor, F.A.; Martínez-Poveda, B.; Quesada, A.R.; Lopez-Crespo, P. High-strength low-modulus biocompatible Nb-1Zr alloy processed by accumulative roll bonding. *Mater. Sci. Eng. A* **2020**, *797*, 140226. [CrossRef]
102. Huo, W.T.; Zhao, L.Z.; Yu, S.; Yu, Z.T.; Zhang, P.X.; Zhang, Y.S. Significantly enhanced osteoblast response to nano-grained pure tantalum. *Sci. Rep.* **2017**, *7*, 40868. [CrossRef]
103. van Wachem, P.; Hogt, A.; Beugeling, T.; Feijen, J.; Bantjes, A.; Detmers, J.; van Aken, W. Adhesion of cultured human endothelial cells onto methacrylate polymers with varying surface wettability and charge. *Biomaterials* **1987**, *8*, 323–328. [CrossRef]

104. Misra, R.D.; Nune, C.; Pesacreta, T.C.; Somani, M.C.; Karjalainen, L.P. Understanding the impact of grain structure in austenitic stainless steel from a nanograined regime to a coarse-grained regime on osteoblast functions using a novel metal deformation-annealing sequence. *Acta Biomater.* **2013**, *9*, 6245–6258. [CrossRef]
105. Rupp, F.; Scheideler, L.; Olshanska, N.; de Wild, M.; Wieland, M.; Geis-Gerstorfer, J. Enhancing surface free energy and hydrophilicity through chemical modification of microstructured titanium implant surfaces. *J. Biomed. Mater. Res. A* **2006**, *76*, 323–334. [CrossRef]
106. Lord, M.S.; Foss, M.; Besenbacher, F. Influence of nanoscale surface topography on protein adsorption and cellular response. *Nano Today* **2010**, *5*, 66–78. [CrossRef]
107. Dheda, S.S.; Kim, Y.K.; Melnyk, C.; Liu, W.; Mohamed, F.A. Corrosion and in vitro biocompatibility properties of cryomilled-spark plasma sintered commercially pure titanium. *J. Mater. Sci. Mater. Med.* **2013**, *24*, 1239–1249. [CrossRef] [PubMed]
108. Wen, M.; Gu, J.F.; Liu, G.; Wang, Z.B.; Lu, J. Surface evolution of a gradient structured Ti in hydrogen peroxide solution. *Appl. Surf. Sci.* **2008**, *254*, 2905–2910. [CrossRef]
109. Cai, K.; Lai, M.; Yang, W.; Hu, R.; Xin, R.; Liu, Q.; Sung, K.L. Surface engineering of titanium with potassium hydroxide and its effects on the growth behavior of mesenchymal stem cells. *Acta Biomater.* **2010**, *6*, 2314–2321. [CrossRef]
110. Shen, X.; Ma, P.; Hu, Y.; Xu, G.; Zhou, J.; Cai, K. Mesenchymal stem cell growth behavior on micro/nano hierarchical surfaces of titanium substrates. *Colloids Surf. B Biointerfaces* **2015**, *127*, 221–232. [CrossRef]
111. Motemani, Y.; Greulich, C.; Khare, C.; Lopian, M.; Buenconsejo, P.J.S.; Schildhauer, T.A.; Ludwig, A.; Koller, M. Adherence of human mesenchymal stem cells on Ti and TiO2 nano-columnar surfaces fabricated by glancing angle sputter deposition. *Appl. Surf. Sci.* **2014**, *292*, 626–631. [CrossRef]
112. Wen, M.; Wen, C.; Hodgson, P.; Li, Y. Improvement of the biomedical properties of titanium using SMAT and thermal oxidation. *Colloids Surf. B Biointerfaces* **2014**, *116*, 658–665. [CrossRef]
113. Ren, B.; Wan, Y.; Wang, G.S.; Liu, Z.Q.; Huang, Y.; Wang, H.W. Morphologically modified surface with hierarchical micro-/nano-structures for enhanced bioactivity of titanium implants. *J. Mater. Sci.* **2018**, *53*, 12679–12691. [CrossRef]